


Progress in the design and modeling methods of the MSC230 superconducting cyclotron for proton therapy

V. A. Gerasimov, S. V. Gursky, O. V. Karamyshev, G. A. Karamysheva*^{}, I. D. Lyapin, V. A. Malinin, D. V. Popov, V. M. Romanov, A. A. Sinitsa, G. V. Trubnikov, S. B. Fedorenko, H. G. Khodzhbagiyani, S. L. Yakovenko, I. M. Palnikov, and A. I. Vlasov

Joint Institute for Nuclear Research, Dubna, Russia

Abstract

With the emergence of the FLASH irradiation method in proton therapy, the need for high-current accelerators has grown significantly. Addressing this demand, the Joint Institute for Nuclear Research (JINR) has initiated the development of the MSC230, a compact isochronous cyclotron designed to produce high-intensity proton beams at 230 MeV for advanced biomedical research. Currently, the technical design of the cyclotron is in progress at D. V. Efremov Institute of Electrophysical Apparatus. Modifications during this phase often necessitate additional calculations, resulting in updates to the magnetic field configuration and beam dynamics. This article details the design methodologies and computational tools employed in the MSC230 project.

Keywords: isochronous cyclotron, magnet, accelerating cavity, beam dynamics

DOI: [10.54546/NaturalSciRev.100404](https://doi.org/10.54546/NaturalSciRev.100404)

1. Introduction

With the advent of the new and promising FLASH irradiation methods [1–3] in proton therapy, the demand for high-current accelerators has significantly increased. This need has driven the development of the MSC230 project at JINR — a compact isochronous superconducting cyclotron designed with a relatively modest central magnetic field strength of 1.7 T. The isochronous cyclotron accelerates a quasi-continuous beam, making it one of the most promising choices for medical applications. The MSC230 is designed to deliver a beam current of approximately 10 μA in short pulses at an energy of 230 MeV, which is sufficient to investigate the efficacy of the FLASH method.

FLASH irradiation achieves a dose rate of over 50 Gy/s in less than 0.5 s, in contrast to conventional radiation therapy, which operates at 1–7 Gy/min. While tumor damage remains identical to that of standard treatment, healthy tissue exhibits greater resistance to FLASH radiation.

*Corresponding author e-mail address: gkaram@jinr.ru

This method has attracted significant interest from specialists as it not only preserves healthy tissue and reduces the number of treatment sessions but also enables the treatment of some radioresistant tumors. The beam current required for irradiating is approximately $10\ \mu\text{A}$ — an order of magnitude higher than in conventional radiation therapy. The upper limit for the beam current in FLASH therapy remains undetermined, though extensive research is underway using proton beams of various intensities. An “extreme” FLASH mode [4] is also explored, involving irradiation of biological objects at a dose rate of $1\ \text{MGy/s}$.

The study of the FLASH method highlights the critical need for a research and innovation center at JINR. Such a facility would include a proton accelerator, an advanced beam delivery system, and cutting-edge laboratory equipment for biomedical research. Below is a brief overview of how the MSC230 project compares to other accelerators used in proton therapy.

1.1. Overview

Proton therapy requires an acceleration of proton beam to energy of 60–230 MeV. That can be achieved using different accelerator technologies. Currently, medical centers primarily use three types of accelerators: cyclotrons, synchrocyclotrons, and synchrotrons. Each type has its own advantages and drawbacks.

Cyclotrons are favored for their reliability and simplicity, as they operate with a constant magnetic field and a fixed-frequency accelerating system. They also offer relatively high beam currents and precise, rapid modulation of beam intensity. However, as cyclotrons produce a beam at a fixed energy, an energy selection system is required to obtain lower energies. This is typically achieved using a degrader, which affects beam quality.

Synchrotrons, despite advantages of high beam quality and the ability to extract beams at different energies, have the drawbacks of significantly lower average beam currents and difficulty to extract the beam current with low fluctuations. Additionally, they require much higher energy of injected beam requiring additional space.

Synchrocyclotrons share similar disadvantages with cyclotrons, but their pulsed acceleration results in lower average beam intensity. However, the development of superconducting synchrocyclotrons has increased their attractiveness due to the possibility of using stronger magnetic fields enabling more compact design. Typically, these devices are significantly smaller and lighter than any other accelerator — for example, the Mevion 250 synchrocyclotron [5] weighs only about 20 t. The trend toward reducing the size and cost of ion beam radiotherapy has driven the success of superconducting synchrocyclotrons, which are particularly well-suited for single-room treatment solutions. However, for full-scale proton therapy centers, isochronous cyclotrons remain the most suitable choice.

To achieve compact dimensions, attempts have been made to develop superconducting isochronous cyclotrons with high magnetic fields of around 3 T, such as the SC200 [6] and Sumitomo 230 MeV [7]. However, these projects faced significant engineering challenges, leading to prolonged development timelines and reduced system reliability.

Thus, while the isochronous cyclotron cannot compete with the synchrocyclotron in terms of compactness, it is significantly better suited for applications requiring high beam intensity.

In proton therapy, two cyclotrons have been particularly successful: the Varian Proscan [8], designed by H. Blosser et al. in 1993, and the C235 (IBA, Belgium) [9]. Both cyclotrons have relatively low central magnetic field strengths of 1.7 and 2.4 T, respectively (see Table 1).

In our project, which parameters are presented in the last column of Table 1, we combine the advantages of both cyclotrons, which presently are leaders in the proton therapy market. From the C235 we took a low magnetic field and the fourth harmonic of acceleration; from the Varian cyclotron we took a superconducting coil, a constant along the radius vertical gap

Table 1. Comparison of key parameters of leading proton therapy cyclotrons and the MSC230 project.

Parameter	Varian Proscan	IBA C235	MSC230
Diameter, m	3.1	4.3	3.86
B_0 , T	2.4	1.7	1.7
Coils	NbTi	copper	NbTi
Weight, t	90	200	130
RF frequency, MHz	72.8	106.5	106.5
RF power, kW	115	60	60
Number of cavities	4	2	4
Harmonic	2	4	4
Energy, MeV	250	235	230
Beam current/pulsed beam current, nA	1000	700	1000/10 000
Number of turns	650	800	500

between the sectors, sufficient to accommodate an electrostatic extraction deflector (ESD) in its wide aperture part, and as a result — four free valleys for placing accelerating cavities.

The low magnetic field together with the high acceleration rate due to usage of four cavities operating at the fourth harmonic result in large turn-to-turn distance and, consequently, efficient extraction by electrostatic deflector. The low magnetic field is advantageous not only for beam extraction and field shimming but also for the superconducting coil design. The technology developed for NICA magnets at VBLHEP is going to be used to manufacture the MSC230 windings. This technology is based on the NbTi wires wound around cupronickel tube with liquid helium flow inside. The coil is located inside a cryostat with an intermediate thermal shield cooled to liquid nitrogen temperature. The space available for the coil enables usage of high-temperature superconducting (HTSC) materials in the future. That can significantly reduce engineering challenges and operation cost.

The main reasons for choosing superconducting coils in the design of the MSC230 are their reduced energy consumption and a relatively compact size of the machine achieved due to smaller winding (even with cryostat accounted). More detailed information on the MSC230 design choices, as well as the justification for the chosen solutions, can be found in [10–12].

1.2. Current status of the MSC230 project

Currently, the technical design of the cyclotron is in progress at D. V. Efremov Institute of Electrophysical Apparatus (NIIEFA). Modifications during this phase necessitated additional calculations, resulting in updates to the magnetic field configuration and beam dynamics. This article presents the methods and results of these new calculations, covering both individual accelerator systems and overall beam dynamics within the cyclotron.

Present status of the main systems of the cyclotron is summarized below:

- SC coils. The technology using a tubular composite superconducting cable, developed at VBLHEP (Veksler and Baldin Laboratory of High Energy Physics, JINR) and well-tested in the magnets of the Nuclotron and Booster synchrotrons, was chosen for manufacturing [13]. The coil production is initiated;
- Magnet status. The 1010-steel ingot was purchased by NIIEFA and the production of the yoke is underway;

- RF power amplifier is being designed by ASIPP (China) and is going to be manufactured by the end of 2025.

2. Main parameters of the MSC230 cyclotron

MSC230 is an isochronous four-sector compact cyclotron with superconducting coils enclosed in a cryostat. All other parts of the cyclotron are “warm”. An internal Penning-type proton source is located at the cyclotron center. Acceleration is performed at the fourth harmonic of the revolution frequency. The radio-frequency (RF) system consists of four cavities located in the cyclotron valleys. Beam extraction is carried out by an electrostatic deflector located in the gap between sectors which is followed by two passive magnetic channels positioned along the extraction trajectory.

Table 2. Main parameters of the MSC230 cyclotron.

General properties	
Accelerated particles	Protons
Magnet type	Superferric — SC coils, “warm” yoke
Injection	Internal source
Number of turns	500
Beam parameters	
Energy, MeV	230
The relative energy spread	0.15%
Extracted beam intensity (continuous mode), nA	2–1000
Extracted beam intensity (flash mode), nA	5000–10 000
Emittances of the extracted beam, $\pi \cdot \text{mm} \cdot \text{mrad}$, (2σ)	
Radial	10
Vertical	5
Magnetic system	
Average magnetic field in the center (R_o)/in the extraction zone (R_{extr}), T	1.7/2.15
Dimensions (height \times diameter), m	1.9×3.86
Magnet weight, t	~ 130
Hill/valley gap, mm	50/700
Excitation current (1 coil), A \cdot turns	290 000
Accelerating system	
Frequency, MHz	106.5
Harmonic number	4
Number of cavities	4
Power losses, kW (total)	60
Voltage per turn center/extraction, kV	40/90
Extraction	
Extraction radius, m	1.08
Extraction system	ESD + 2MC

3. Virtual prototyping

In a compact cyclotron, spatial constraints create contractional requirements among systems. An integrated design approach is essential to ensure that the design decisions balance the requirements of all systems. Virtual prototyping plays a key role in this process, enabling the seamless development of a cyclotron from the conceptual phase to the technical design stage.

The core idea of the engineering methodology called Virtual Prototyping is to replace physical mock-ups with integrated software prototypes. These prototypes incorporate functional simulations based on CAD techniques. We have developed a framework in MATLAB to integrate the individual systems of the cyclotron. The shapes of the magnet sectors and cavities are initially selected within MATLAB. These parameters are then exported to CAD software (SolidWorks) to create a parameterized model of the cyclotron. Subsequently, individual systems are simulated in CST Studio Suite using its specialized modules. Results of electromagnetic field calculation from CST are re-imported into MATLAB for analysis on the closed equilibrium orbits with the CORD code [14] and beam-tracking simulations.

Comprehensive calculations of beam dynamics are performed for critical regions, such as the central zone (injection) and the extraction region. Based on the analysis, iterative structural modifications are made to the cyclotron systems. This process is repeated until the desired outcome — successful beam injection, acceleration, and extraction — is achieved.

3.1. The reasoning behind opting for a top-down design approach

The design process began by defining the main requirements for the entire system. Then, the logical architecture of the entire structure has been defined by the system's main functions. This top-down approach has been chosen to create the key components of the cyclotron, the magnetic and accelerating systems. These components are designed in the context of the entire system to simplify the process of making changes at the assembly level. Bottom-up approach is more suitable for standard parts, where each part can be designed independently (for example, beam probes, ion source). The bottom-up approach was traditionally used for cyclotron design; however, it often causes engineering difficulties during the integration phase. It should be noted that any practical design process still requires multiple iterations, resulting in a combination of these two basic approaches.

A preliminary three-dimensional model of the cyclotron with its subsystems was produced using a top-down modeling method in the CAD software (SolidWorks) and simulated in the CST studio environment provided by Dassault Systèmes¹. The 3D modeling key aspects define the position of all subsystems and their interfaces in the available space and parameterize them. The model allows for quick implementation of modifications with the required checks of compliance with mechanical, electrical, and thermal requirements after multiple iterations between the geometrical modeling environment and several multiphysics simulation environments.

3.2. Virtual prototyping of key components

Following the selection of the main parameters for all major systems based on modeling results, the next step is the detailed design of individual systems for manufacturing. In the next sections, we will go over the development of the radio frequency (RF) system, vacuum

¹However, to ensure the accuracy and reliability of the results, we regularly perform verification by comparing them with the data obtained using other software, such as Comsol and Tosca.

system, and magnetic system. In the process we use CST's Magnetostatic and Electrostatic solvers, the RF Eigenmode module, and Conjugate Heat Transfer module.

3.2.1. Design of radio frequency system

The MSC230 cyclotron's accelerating system is comprised of four half-wave cavities that have D-electrodes and are connected in the center, with two stems attached to ensure sufficient structural rigidity. The RF cavities are positioned in the magnet valleys, with their geometry constrained by the size of the spiral sectors.

For proton acceleration, we opted for four RF accelerating cavities operating in the fourth harmonic mode. The choice of the fourth harmonic is natural for a cyclotron with four sectors and ensures a high acceleration rate. All four cavities operate at a frequency of approximately 106.5 MHz.

Depending on the requirements, the Eigenmode module employs different numerical methods to calculate eigenmodes. The finite element method (FEM) is more accurate for complex geometries, while the finite integration technique (FIT) is better suited for rapid calculations of large structures. The Eigenmode module allows users to visualize fields for various modes, helping developers to understand how fields are distributed and interact within the device. The module can account for lossy materials (e.g., finite conductivity or absorption in dielectrics) and calculate the quality factor (Q-factor) of resonant structures, which is critical for evaluating energy losses and resonance width.

One of the key parameters of the accelerating system is the dependence of the accelerating voltage on the radius (see Fig. 1). To characterize this dependence, we calculate the integral of the electric field vector, \mathbf{E} , along an arc from the middle of cavity A to the middle of sector B in the median plane at the time of maximum electric field, which yields the voltages for the input and output gaps:

$$V_{AB} = \int_A^B \mathbf{E} \cdot d\mathbf{l}.$$

The Eigenmode module is sufficient for addressing the key tasks in designing RF cavities. The tasks include computation of eigenfrequency, optimization of accelerating voltage distribution along the radius, and minimization of power losses. Additionally, a detailed thermal analysis of the cavities is also crucial for evaluating RF system performance. This can be done

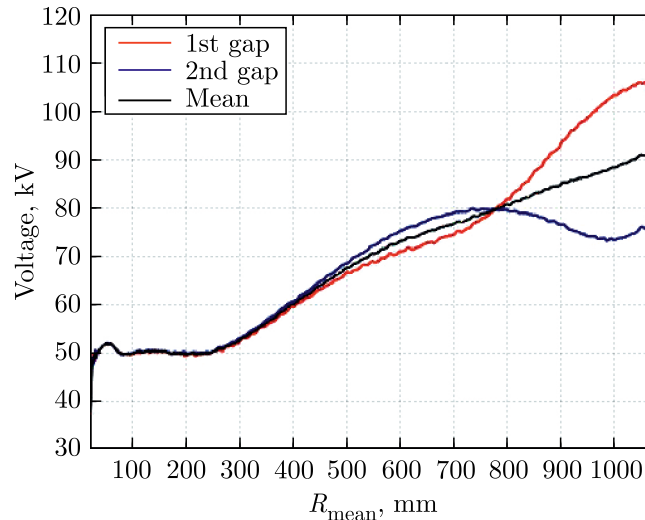


Figure 1. Dependence of accelerating voltage per gap on the orbit radius.

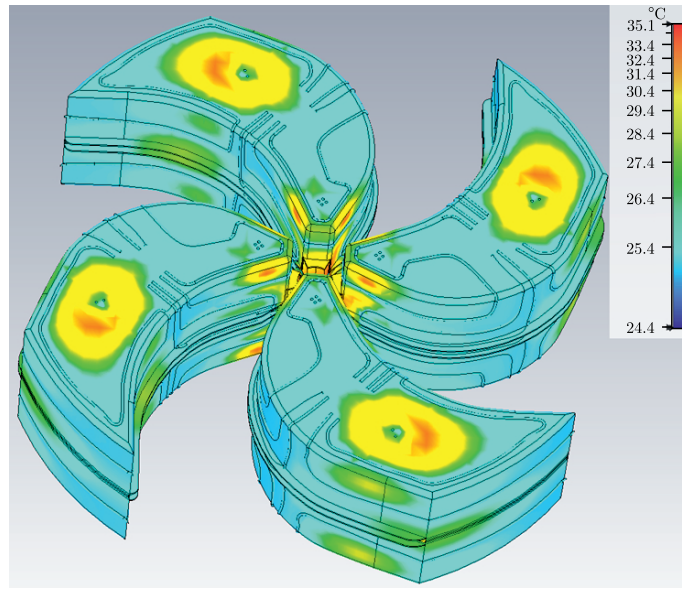


Figure 2. Liner heating visualization performed in CST Studio.

using the Conjugate Heat Transfer (CHT) Solver module, which plays a vital role in the cooling system design. Reduction of heat power density on the cavity walls is essential for the design of cavity cooling. The heat distribution on cavity walls determines requirements for cavity cooling which has to prevent excessive temperature increase of cavity walls and related to it cavity deformation and detuning. That ensures the cavity stable and reliable operation thereby enhancing the performance of the RF system (see Fig. 2).

The calculated average power loss is approximately 60 kW for the storage energy 1 J and the voltage distribution presented in Figure 1. The particles will be accelerated at a central voltage of about 40 kV/gap. Since the real resonator's quality factor is usually 20–30% lower than the simulated one, the total losses are expected to stay less than 60 kW. The maximum beam loading of 2.3 kW is negligibly small. It causes only a proportional increase in the number of turns required in the accelerator.

3.2.2. Vacuum system

The vacuum system of the MSC230 cyclotron includes three major parts supporting: isolating vacuum of SC coil located in a cryostat, vacuum in the cyclotron main chamber and vacuum in an internal ion source. The most challenging requirement is for the vacuum system of the cyclotron vacuum chamber. To support reliable operation of the RF system, a residual gas pressure in the chamber has to be better than 2×10^{-5} mbar under normal operational conditions [15].

The primary gas load originates from the hydrogen ion source which sets quite high requirement for pumping speed. Shimadzu TMP-2804LM turbomolecular pump was chosen for pumping the cyclotron chamber. It has pumping speed of 2300–2800 L/s for nitrogen and 1700–2000 L/s for hydrogen. Four such pumps are required to obtain the required vacuum. Two of them are above the upper yoke and two below the lower yoke.

To validate this choice, vacuum simulations were carried out using Comsol. Their results indicate that to achieve the required pressure in the vacuum chamber the pumps have to be placed near the surface of the yoke. To have sufficient margin guarantying good vacuum conditions, we increased in the simulations (1) the gas flow coming from the ion source from the design value of 3.33×10^{-2} mbar · L/s to 6.67×10^{-2} mbar · L/s, and (2) the desorption

load from the vacuum chamber walls and resonance system from 3.78×10^{-3} mbar·L/s to 1.68×10^{-2} mbar·L/s. Calculations show that the pressure still remains within the 10^{-5} mbar range. That is sufficient for achieving the design goal.

3.2.3. Design of magnet system

The main characteristics of the magnet are:

- four-fold symmetry and spiral sectors;
- deep-valley concept with RF cavities placed in the valleys;
- stray magnetic field is about 200 G near the accelerator.

The magnet sectors of the cyclotron consist of two parts:

- a wide-aperture part with a vertical distance of 50 mm;
- a small-aperture part with a vertical distance of 25 mm.

This structure, combined with a chamfer along the beam trajectory, yields an isochronous magnetic field up to radii of beam extraction. The wide-aperture part allows one the placement of electrostatic deflector. The effectiveness of such a sector structure has been demonstrated in [12].

Simulations of the magnet were performed in CST studio (see computational model and magnetic field distribution in Fig. 3). The magnetic field of the MSC230 is formed by iron. Magnetic field along radius (azimuth 0 degrees) is shown in Fig. 4. The average magnetic field and flutter of the developed model are shown in Fig. 5. Flutter characterizes the depth of the azimuthal variation of the magnetic field:

$$F(r) = \frac{\bar{B}^2 - \bar{B}^2}{\bar{B}^2}.$$

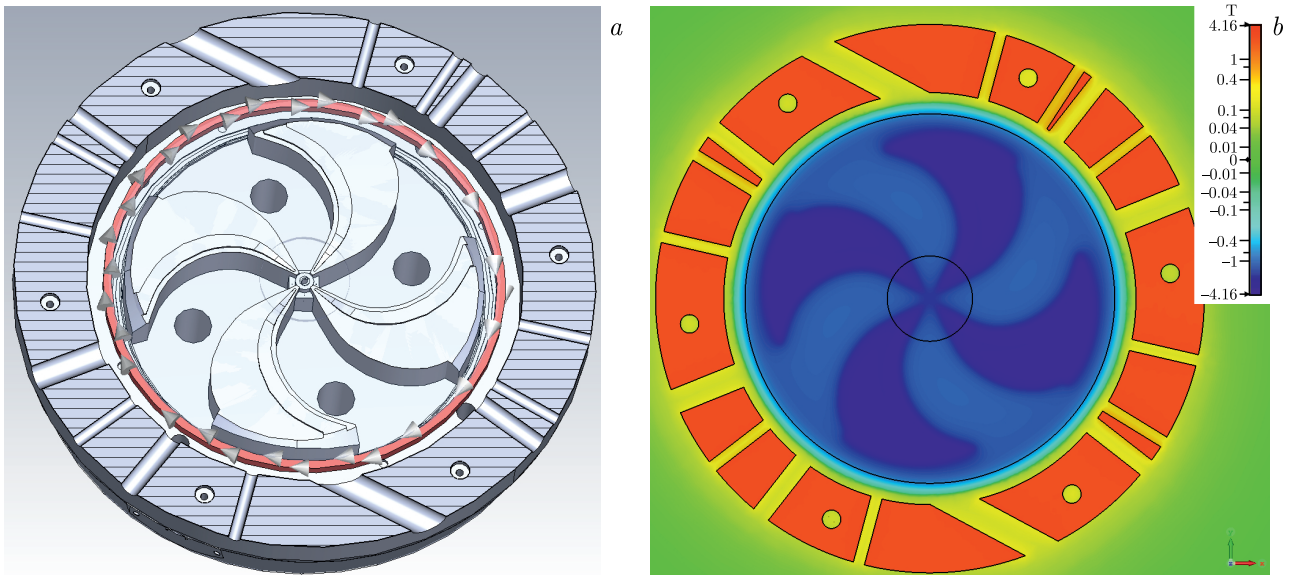


Figure 3. a) Cyclotron magnet configuration (computational model). b) Magnetic field distribution in the median plane.

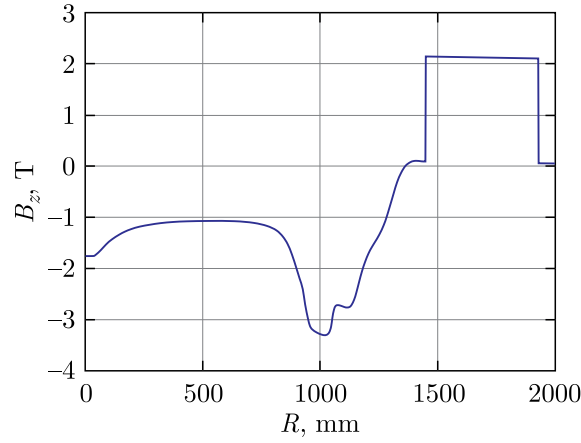


Figure 4. Magnetic field along radius (azimuth 0 degrees).

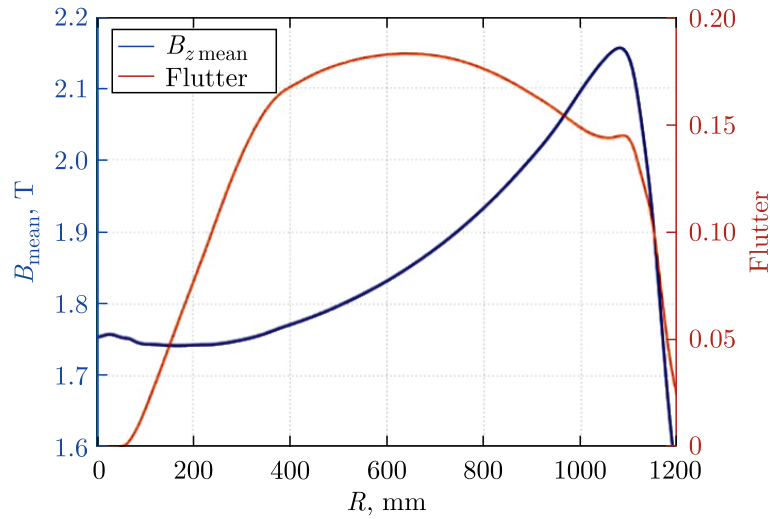


Figure 5. Mean magnetic field and flutter vs radius.

Since there are four poles in the magnet, the dependence of ideal magnetic field on the azimuth has to include harmonics with numbers $4n$ only, where n is an integer. However, practical magnet has considerable deviations from the ideal one. The lowest three harmonics of the magnetic field are shown in Fig. 6. The presence of the second harmonic of the magnetic field in the center is determined by the shape of the central plug. The values of low number harmonics are smaller than 5 G in the extraction region. High flutter (see Fig. 5) minimizes the spiral angle of the sector shims. The flutter and spiral shape of the sectors provide the vertical focusing necessary for the beam acceleration.

3.3. Particle dynamics analysis

The design of a cyclotron relies on two distinct aspects of particle dynamics: the analysis of closed equilibrium orbits and the simulation of particle trajectories under acceleration (beam tracking).

The former is adequate for defining the global magnet design including the size and shape of the sectors and the average field. Known geometry of the magnet determines the space

available for cavities while their geometry and design are set by the voltage distribution along the radius and the RF frequency.

The latter, however, is necessary for modeling the beam's behavior during acceleration in the central region and throughout the extraction process.

3.3.1. CORD

CORD (Closed ORbit Dynamics) is a program designed for analyzing magnetic field and accelerating field maps on equilibrium closed orbits. The software provides comprehensive data on the average and isochronous fields, lower and multiple harmonics of the magnetic structure (Fig. 6), particle rotation frequency as a function of radius (Fig. 7), and betatron oscillation frequencies (see Fig. 8).

The analysis of the accelerating field yields information about the azimuthal extent of cavities, distribution of accelerating voltage along the radius, maximum energy gain per turn, orbit step, number of turns, and calculation of the phase motion of the central particle.

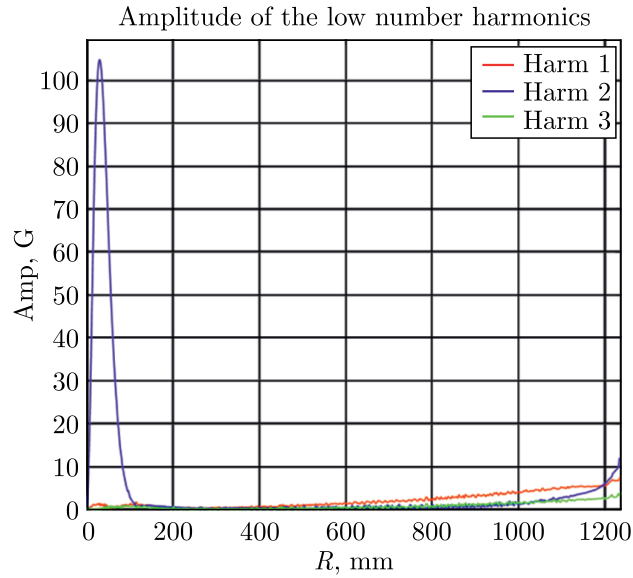


Figure 6. Dependences of amplitude of magnetic field harmonics on the radius for the first three harmonics.

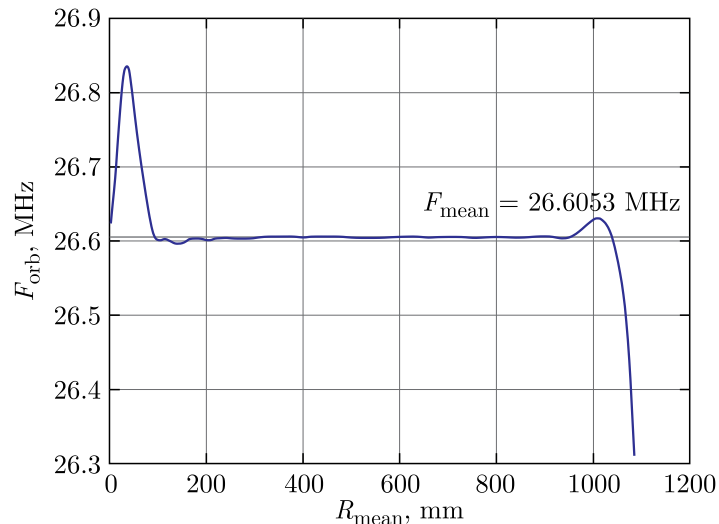


Figure 7. Orbital frequency compared to the mean one.

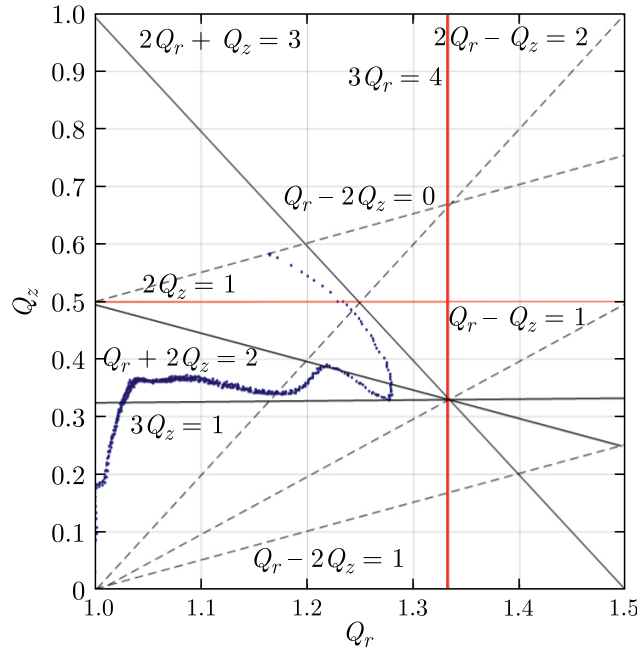


Figure 8. Tune diagram.

3.3.2. Beam tracking

After constant energy calculations are done and the magnet and cavity designs are optimized, one needs to do calculations of the entire acceleration. In our study of beam dynamics, we traditionally utilize a three-dimensional magnetic field map of the magnet system and electromagnetic field maps of the accelerating system. Electromagnetic field maps are obtained through eigenmode calculations of cavities using CST Studio Suite. This approach is particularly crucial for designing cyclotrons with spiral sectors and cavities. The primary reason lies in the significant variation of the accelerating voltage along the radius.

Initial acceleration

The most important characteristic of the beam at the exit from the central zone is the amplitude of the radial betatron oscillations of the particles (see Fig. 9). The magnitude of the amplitudes of the radial oscillations of the particles can be used to judge the degree of beam centering. Precision calculation of beam dynamics would seem to allow the central region to be formed in such a way as to ensure good beam centering.

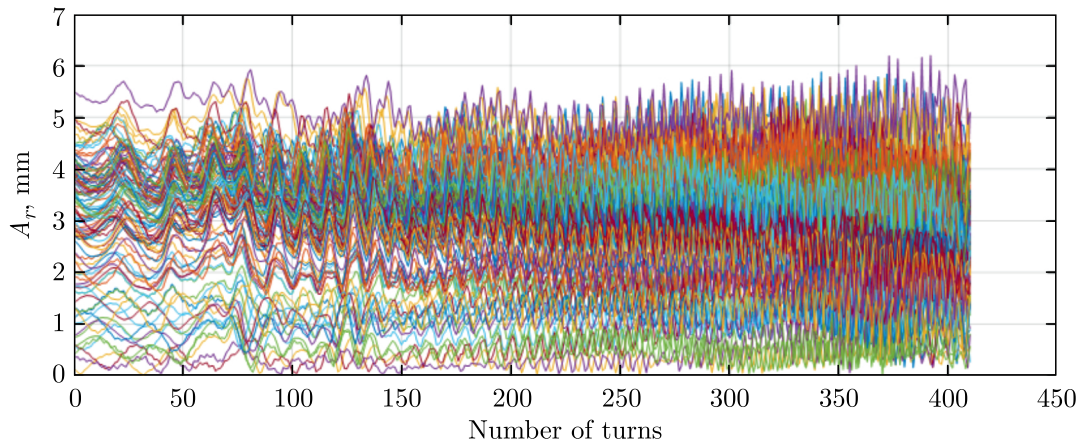


Figure 9. The amplitudes of the radial oscillations of the particles.

Figure 10 presents the betatron oscillation frequencies at the cyclotron center. Magnetic focusing is observed to commence at a radius of approximately 40 mm, which corresponds to the beam's third turn. For radii less than 40 mm, vertical focusing is provided by the accelerating electric field for particles that are lagging in RF phase.

In Figure 11, white dots indicate the locations where protons collide with elements of the cyclotron structure, marking the points of beam loss. Green and yellow dots represent the positions of particles when the electric field reaches its maximum. Green dots correspond to particles that passed through the central region, while yellow dots denote those lost later. The transmission coefficient through the central region was computed for particles accelerated through four turns and amounted to about 20% of the particles occupying a 180-degree RF accelerating field. The histogram of particles phases passing through the central region is shown in Figure 12.

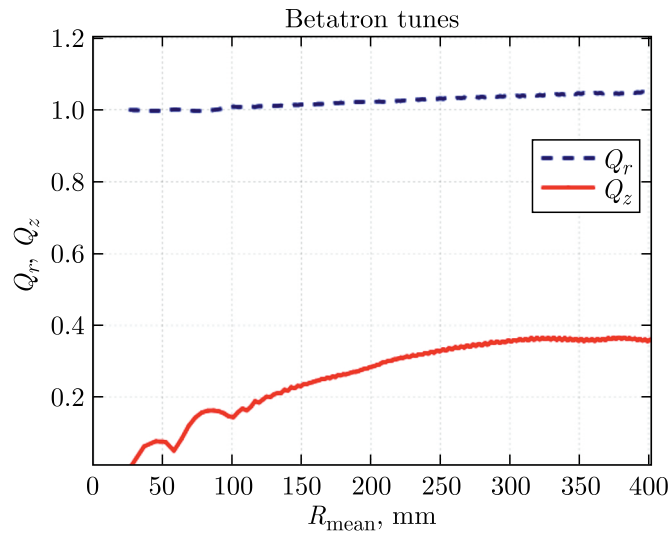


Figure 10. Betatron frequencies against radius of closed orbit in the central region.

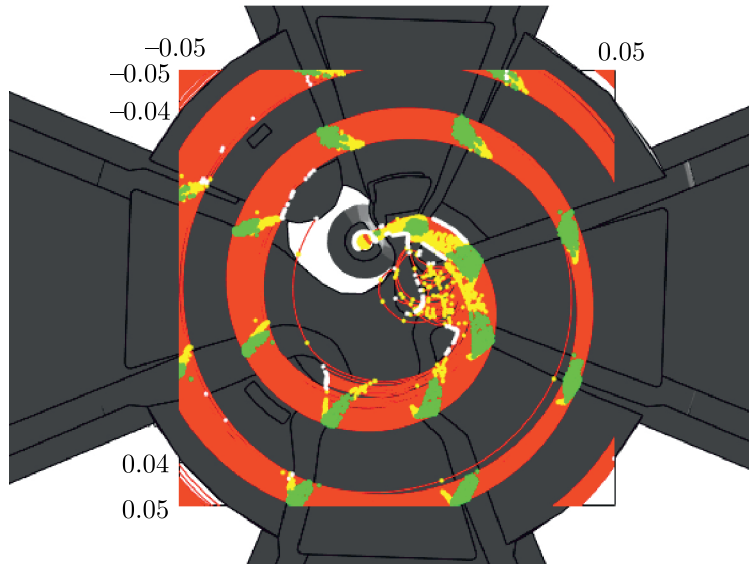


Figure 11. Beam trajectories in the central region (red).

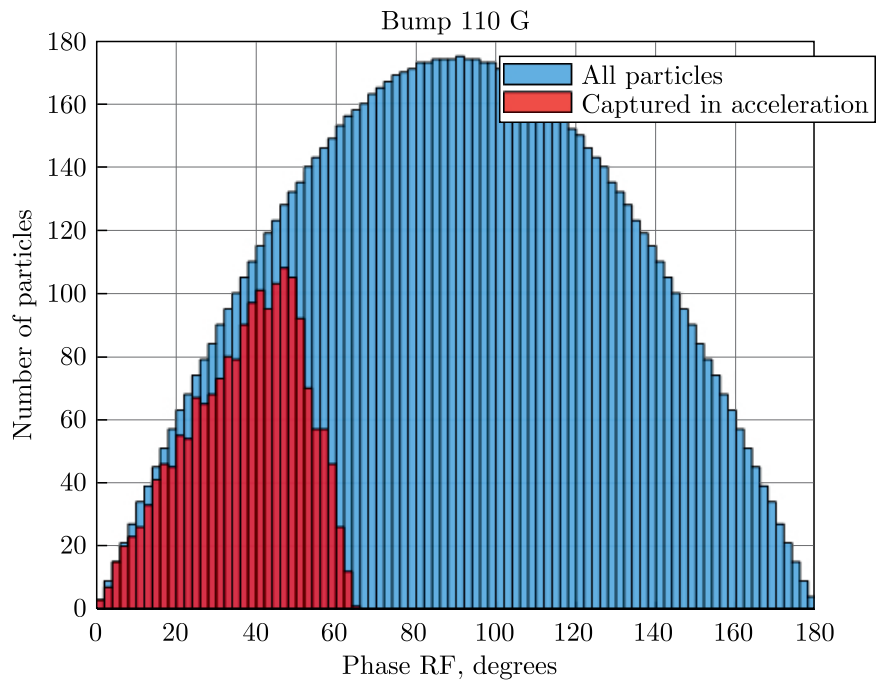


Figure 12. Particle distribution over accelerating phase for 10 000 initial particles (blue) and particles captured in acceleration (red).

Acceleration zone

After optimization of initial acceleration, we simulated the beam acceleration from the ion source to the energy of 230 MeV. Results of simulation are presented in Figures 13–15 below.

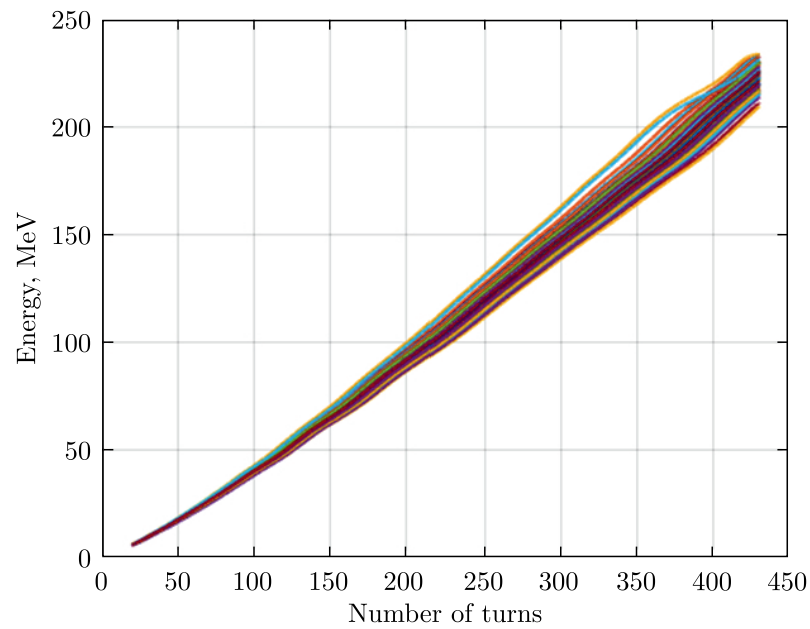


Figure 13. Energy of the accelerated particles against the turn number.

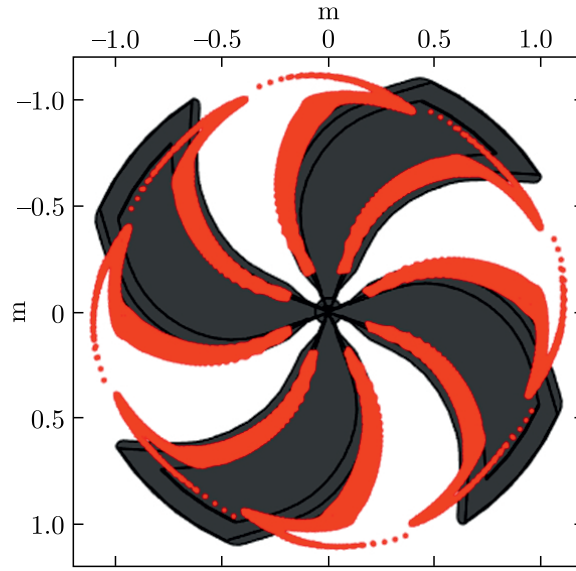


Figure 14. Particles position every 180 degrees RF (at the moment of the maximum value of electric field).

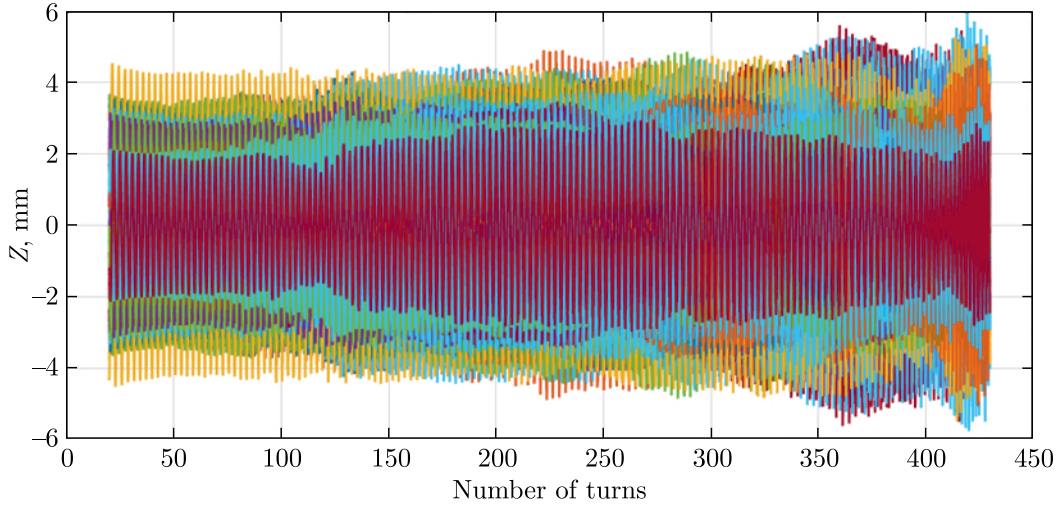


Figure 15. Vertical motion of the beam.

Beam extraction

A low magnetic field in combination with a high acceleration rate creates a possibility of effective beam extraction using an electrostatic deflector (ESD) located between the sectors and two passive focusing magnetic channels [16]. We limit the electric field in the deflector to 100 kV/cm. The beam, deflected by ESD, first passes through one accelerating RF cavity, then through a magnetic channel (MC1) located between the magnet sectors, then through a second accelerating RF cavity (see Fig. 16). After traversing a second magnetic channel (MC2) between the next sectors, it exits the cyclotron, thus completing half a turn. The first magnetic channel reduces the average magnetic field by 1400 G and provides a gradient of 700 G/cm, the second one provides a gradient of 2500 G/cm.

All particles from the beam that pass through the central region reach the deflector entrance. Approximately 15–20% will be lost on the deflector septum (assuming a thickness of 0.15 mm) when the deflector perfectly aligns with the beam orbit. In a perfectly isochronous

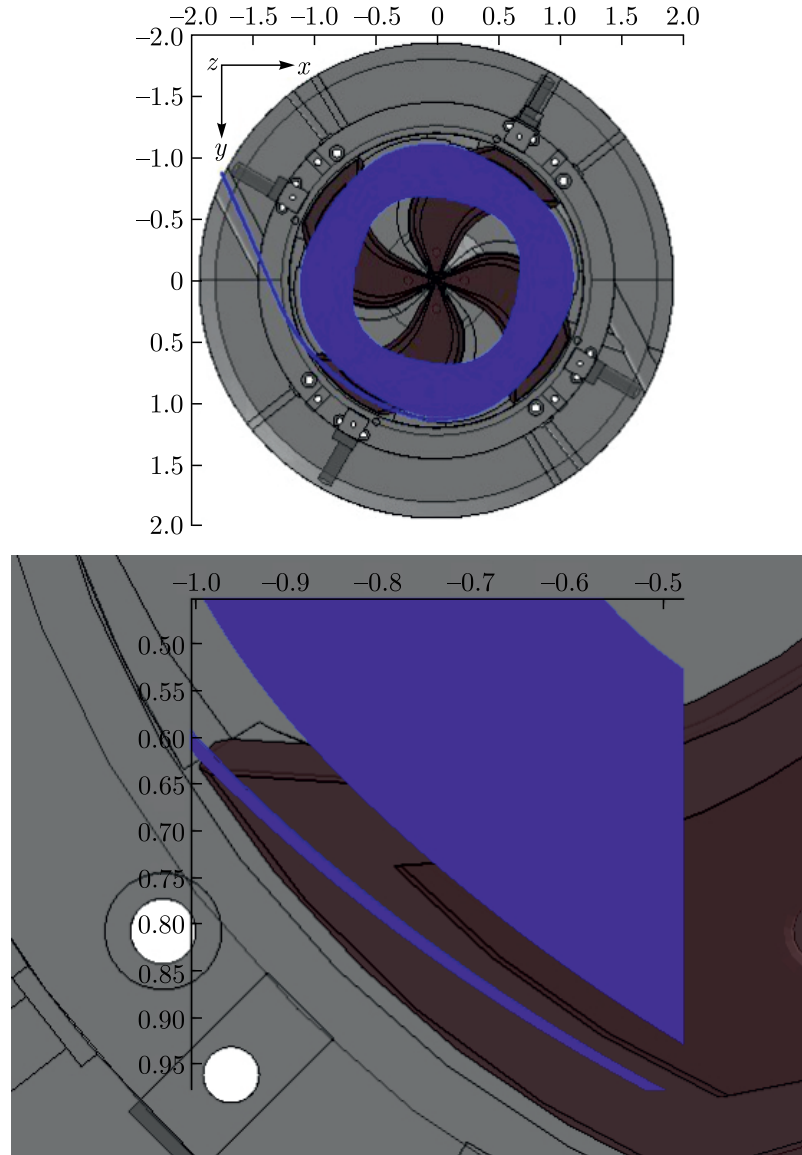


Figure 16. Beam extraction.

cyclotron, an RF phase of the particle remains constant during acceleration, leading to multi-turn extraction. Since particles with different initial RF-phase values complete a different number of revolutions before reaching their final energy and being extracted by the ESD, the turn count varies. In our cyclotron, for example, the number of turns can differ by up to 50, with a total of around 500.

The calculated horizontal emittance at the accelerator exit is about $10 \pi \cdot \text{mm} \cdot \text{mrad}$, and the vertical emittance is about $5 \pi \cdot \text{mm} \cdot \text{mrad}$.

4. Testing individual systems of the MSC230 cyclotron

For the successful launch of the MSC230 cyclotron, testing of prototypes of individual systems is required. Several systems, primarily the ion source and deflector, have finite lifetime and will need replacement during operation. For the ion source, a key task is its optimization aimed at increasing the intensity of the extracted beam and the source lifetime. The voltage at the ESD required for beam extraction is about 90–100 kV/cm. The thickness of the cyclotron

deflector septum is directly related to the beam loss at the extraction, which may limit the maximum beam current. The minimum thickness of the septum depends on the material and manufacturing technology.

Testing the ion source and deflector will help establish optimal designs and improve their performance characteristics.

5. Conclusion

This article has presented the integrated design and modeling methodology employed in the development of the MSC230 superconducting cyclotron. The iterative approach, combining top-down architecture definition with high-fidelity simulations in CST Studio Suite, followed by beam dynamics simulations, has been crucial for optimizing the system.

The results demonstrate that the MSC230 cyclotron is expected to deliver a beam current that exceeds that of presently operating accelerators in its class. This increase in beam intensity is achieved through a novel combination of a comparatively low magnetic field with a high accelerating rate, ensuring minimal energy consumption. Furthermore, high beam intensity should be reached by an efficient internal ion source and an optimized central region for beam formation.

In summary, the advanced design and modeling methods applied here have proven highly effective in developing a next-generation cyclotron that promises significantly enhanced performance for proton therapy applications, paving the way for more efficient and accessible cancer treatment.

Conflicts of interest

The authors declare no conflicts of interest.

References

- [1] A. A. Patriarca, FLASH radiation therapy: Accelerator aspects, in: Proceedings of the 11th International Particle Accelerator Conference (IPAC 2020), Caen, France.
- [2] S. Jolly, Y. Owen, M. Shipper, C. Welsch, Technical challenges for FLASH proton therapy, *Physica Medica* 78 (2020) 71–82.
- [3] <https://www.appliedradiology.com/articles/varian-first-patient-treated-in-fast-01-flash-therapy-trial>
- [4] S. V. Akulinichev et al., Potential of proton FLASH therapy on the accelerator of the Institute for Nuclear Research of the Russian Academy of Sciences, *Izvestiya RAN. Series Physics*, 84 (11) (2020) 1544–1548 (in Russian).
- [5] <http://www.mevion.com/products/mevion-s250-proton-therapy-system>
- [6] G. Karamysheva et al., Present status of the SC202 superconducting cyclotron project, VIIIth International Particle Accelerator Conference (IPAC 2017), Copenhagen, Denmark, THPVA120.
- [7] H. Tsutsui et al. Current status of Sumitomo's superconducting cyclotron development for proton therapy, *Cyclotrons 2019*, Cape Town, FRA02, pp. 340–343.
- [8] J. Schippers, R. Dölling, J. Duppich, G. Goitein, M. Jermann, A. Mezger et al., The SC cyclotron and beam lines of PSI's new proton therapy facility PROSCAN, *Nuclear Instruments and Methods B* 261 (2007) 773.
- [9] D. Vandeplasche et al., Extracted beams from IBA's C235, in: Proceedings of Particle Accelerator Conference, Vol. 1, 1997.

- [10] O. Karamyshev et al., Research and development of the SC230 superconducting cyclotron for proton therapy, *Physics of Particles and Nuclei Letters* 18 (1) (2021) 63–74.
- [11] K. S. Bunyatov et al., Progress in design of MSC230 superconducting cyclotron for proton therapy, 23rd International Conference on Cyclotrons and Their Applications (CYC2022), Beijing, China, THPO012, p. 327.
- [12] O. V. Karamyshev, Beam dynamics in a new 230 MeV cyclotron, 23rd International Conference on Cyclotrons and Their Applications (CYC2022), Beijing, China, WEPO003, p. 208.
- [13] H. G. Khodzhibagiyan et al., Development of superconducting accelerator magnets at JINR, *Natural Science Review* 1 (6) (2024).
- [14] O. Karamyshev et al., CORD (Closed Orbit Dynamics): A new field map evaluation tool for cyclotron particle dynamics, *Physics of Particles and Nuclei Letters* 18 (4) (2021) 481–487.
- [15] M. Palnikov, Calculation of pressure distribution in the vacuum chamber of the MSC-230 cyclotron, Master's Thesis, Dubna University, 2024 (in Russian).
- [16] D. Popov et al., Beam extraction simulation and magnetic channels' design for MSC230 cyclotron, 23rd International Conference on Cyclotrons and Their Applications, 2022, Beijing, China, THAO02.